INVITED PAPER

Multiscale Modeling of Charge and Energy Transport in Organic Light-Emitting Diodes and Photovoltaics

The operation of organic LEDs and photoelectric devices can be simulated by combining models at molecular levels with modeling on a scale visible to the naked eye.

By Alison B. Walker

ABSTRACT | Modelling organic devices is an outstanding challenge because device performance is very sensitive to how the molecules are packed and the films are highly disordered. An understanding of charge and exciton (bound electron-hole pair) transport in these materials is important if organic light-emitting diodes are to be exploited in displays, lighting, photovoltaics, transistors, and sensors. This paper discusses methods we have pioneered for predicting charge and exciton transport, in which polymer chains are explicitly modeled and charge and exciton transfer rates are taken from electronic structure theory. Monte Carlo and drift diffusion device models that link device performance with morphology are also covered. The focus here is on polymers, but there is much in common with small molecule organic materials.

KEYWORDS | Charge carrier mobility; diodes; displays; energy conversion; excitons; modeling; photovoltaic cells; plastic films

I. INTRODUCTION

The field of organic or plastic electronics started in the 1950s with the discovery that some organic molecules (i.e., molecules using the same elements as in biological systems, notably carbon and hydrogen) are electroluminescent and the subsequent realization that some of them can act as electrical conductors.[1] The first OLED was reported in 1987 [1] and was based on small molecules. OLEDs employing polymer chain molecules were first demonstrated in 1990 [2]. OLEDs are being developed for television screens, computer displays, cell phones, keyboards and more recently to photoluminescence-based chemical and biological sensors [3]. A significant benefit of OLED displays over traditional liquid crystal displays is that OLEDs do not require a backlight to function so draw less power and are much thinner. OLEDs can be used in large-area light-emitting elements since they typically emit less light per area than inorganic solid-state based LEDs, which are usually designed for use as point-light sources. While some commercial applications are starting to appear, notably in small screens for mobile phones and portable digital audio players, organic devices are still some years away from full exploitation. Additional advancements are needed in light output, color, efficiency, cost, and lifetime.

Active matrix displays employ thin film transistors (TFTs). Organic TFTs have many additional applications such as radio-frequency identification [4] and as light-emitting devices [5]. Organic electronics allows the possibility of unconventional commercial products such as flexible, wearable, disposable electronics, but as for OLEDs, further application of the technology is hindered by poor speed, power consumption, and manufacturability.

Manuscript received September 6, 2008; revised April 3, 2009. Current version published August 14, 2009. This work was supported by the European Commission under STREP project MODECOM NMP-CT-2006-016434, the U.K. Engineering and Physical Sciences Research Council, the Royal Society, and Cambridge Display Technology.

The author is with the Department of Physics, University of Bath, Bath BA2 7AY, U.K. (e-mail: a.b.walker@bath.ac.uk).

Digital Object Identifier: 10.1109/JPROC.2009.2023810

[1]A good summary of organic light-emitting diode (OLED) technology can be found at http://www.en.wikipedia.org. For up-to-date information about applications and many excellent technical reviews, consult Web sites such as www.oled-info.com, www.idtechex.com, and those of the firms exploiting this technology.

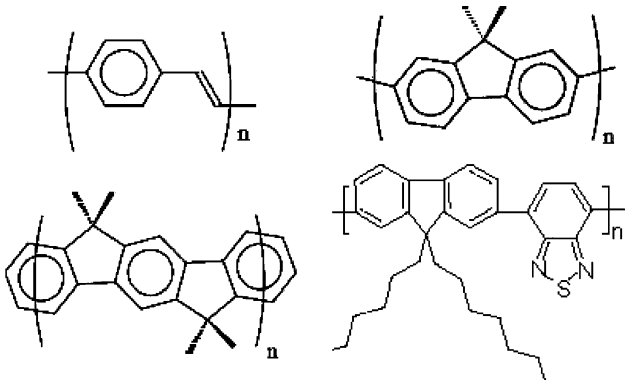

Fig. 1. *Structures of (top left) poly-(p-phenylenevinylene); (top right) PFO; (bottom left) polyindenofluorene (PIF); and (bottom right) F8BT.*

By inverting the OLED operation to generate current from light input, the same organic materials can be used as photovoltaic devices [6], [48] and light detectors. The long-term aim is to develop integrated circuits containing organic LEDs, sensors, TFTs, and photovoltaics that can be made on flexible substrates by cheap large scale roll-to-roll processing described in the many Web sites that cover organic devices.

Small molecule OLEDs have longer lifetimes than polymer OLEDs, and the technology is more advanced. However, small molecules often require vacuum deposition, whereas light-emitting polymers have the major advantage that they are soluble and therefore can readily be deposited in solution onto a display substrate by, e.g., spin-coating or inkjet printing. Hybrid OLEDs in which polymers are combined with emissive guest molecules or inorganic quantum dots are therefore becoming popular.

Semiconducting organic molecules are conjugated, namely, their atoms are covalently bonded with alternating single and multiple (e.g., double) bonds. The chemical structures of some widely used polymers are shown in Fig. 1. The side chains, e.g., C_8H_{17} for poly-(9,9-dioctylfluorene) (PFO), do not conduct and are there to provide solubility and control the packing. Many polymer OLEDs employ copolymers in which two or more different monomers are part of the same polymer chain. An example is poly(9, 9′—dioctylfluorene-co-benzothiadiazole) (F8BT), where the BT monomer is an electron transporter and the F8 monomer a hole transporter. Compared with previous approaches based on polymer blends, this copolymer approach avoids problems associated with phase-separation phenomena in the active layer of OLEDs [7].

The operation of a single-layer OLED is shown in Fig. 1. The thickness of an OLED is typically 10–100 nm. A voltage is applied across the OLED such that the anode is positive with respect to the cathode. Thus, the cathode injects electrons into the organic layer and the anode withdraws electrons from or equivalently injects holes into the organic layer. The key processes in OLEDs are charge injection; electron and hole transport; recombination resulting in exciton (bound electron-hole state) formation; energy transfer by exciton diffusion; and light emission from radiative decay of excitons. Recombination takes place over a region, the recombination zone, whose width is primarily determined by the electron and hole density overlap but that is smeared by diffusion of the excitons between formation and emission. For efficient operation, radiative recombination should take place away from the electrodes to reduce quenching by surface plasmons and degradation caused by impurity diffusion from the electrodes; thus most OLEDs have several layers.

Electrons and holes each have spin 1/2, so triplet (three-state) and singlet (one-state) excitons result from the recombination of electrons and holes. Singlets can decay radiatively on a time-scale of nanoseconds but triplet radiative transitions are forbidden in fluorescent molecules. Thus the singlet: triplet ratio, the fraction of excitons created as singlets as opposed to triplets, limits OLED efficiency. If the charge-transfer configurations that are the immediate precursors of the luminescent states in OLEDs are formed from electrons and holes with a random distribution of spin symmetry, three triplet charge-transfer states will be formed for each singlet charge state, so the maximum possible OLED efficiency would be 25%. Studies of these charge-transfer states in organic dyes and oligomers have shown that the singlet-triplet energy gap associated with these states depends strongly on the molecules involved and their relative orientation. This energy gap affects singlet formation efficiencies; thus the materials and geometry can play a crucial role in determining singlet-triplet ratios and the fluorescence efficiency of a given device [8]. Spin orbit coupling interactions between electron spin and orbital angular momentum allow triplets to emit by phosphorescence on a time-scale of milliseconds and can convert singlets to triplets. This effect is strong in heavy atoms such as iridium. It has been used in white OLEDs [9]. Other nonradiative decay channels, e.g., via defects, can also reduce efficiency.

In polymer devices, the morphology, i.e., packing arrangement of the molecules, has a major impact on device characteristics [10], [11]. Deposition from solution creates

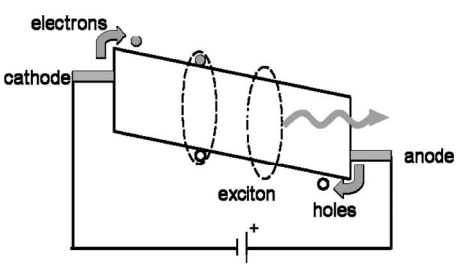

Fig. 2. *Schematic diagram of OLED operation.*

a highly disordered system involving one-dimensional (1-D) structures (chains), two-dimensional (2-D) structures (lamellae), and energetic disorder. The mechanism by which charges [12] and excitons [13], [14] move along a chain backbone (intrachain motion) is different from that for movement between chains (interchain motion), so dimensionality is critical to understanding transport in polymers. The distance between chains is less than 1 nm, so charge and exciton transport in devices involves transfer between a large number of molecules. A theoretical analysis must allow for electronic structure, morphology, and the interplay between different types of disorder on an equal footing. Percolation can play an important role, but the sensitivity to morphology means that standard statistical mechanical models for disordered systems are not always helpful for these systems.

Therefore it is necessary to study how the organization and structural properties of organic materials determine the transport properties of charge carriers and excitons, especially in the device architectures needed for technologies exploiting organic materials. To address charge [12] and exciton [14] transport in polymers, we have pioneered a multiscale approach involving explicit modelling of polymer chains on the mesoscale (1–10 nm) and charge-transfer rates from electronic structure theory, which concerns interactions between nuclei and electrons on microscopic length-scales. The charge mobilities and exciton diffusion coefficients are critical parameters in device models we have developed, based on dynamical Monte Carlo methods at the mesoscale and continuum models at a macroscopic length scale.

This paper focuses on this approach with reference to relevant work by others. I have described these models in the context of OLEDs, except for the device modeling described in this paper that has so far focused on organic photovoltaics. Our work is also relevant to organic TFTs [4] and ambipolar ligh-emitting transistors (OLETs) [5] since slow carrier mobilities translate into sluggish response times. An active display is therefore unable to render motion. This paper is not intended to be exhaustive and will focus on polymers, as we have developed our model with polymers in mind. There are many issues in common with small molecule organic devices; however, excellent reviews of charge transport in molecular materials have recently appeared [15], [16].

We have considered an idealized morphology since simulations of the morphology using intermolecular potentials from first principles potentials coupled to charge transport simulations from electronic structure, apart from a recent calculation of electron states in amorphous polyfluorene [17], have so far been done only for stacked small molecules [18], [49] and are restricted to small systems. A model of charge transport in a disordered small molecule organic solid that explicitly considers the packing and electronic structure of individual molecules has also been developed [19].

In Section II, a brief outline is provided of charge and energy transport mechanisms in organic materials. In Sections III–V describe, respectively, our multiscale modeling methods of charge and energy transport and our device models. Section VI concludes this paper.

II. CHARGE AND ENERGY TRANSPORT MECHANISMS

A short summary of the basic ideas will be provided here as background to the multiscale modeling approach we have developed in [12] and [14]. The molecular conformation, namely, the geometry of the polymer as defined by the coordinates of the atomic nuclei, depends on the environment (vacuum, solvent, etc.). Adding an electron or hole to a molecule changes its conformation as atomic positions adjust to minimize the total energy. In the process, molecular orbitals and energy levels change. At room temperature, the energy gained by localizing charge carriers to groups of typically three monomers termed conjugated segments, and from the increased polarization of the surrounding medium, exceeds the energy gained by charge delocalization along a polymer chain, leading to self-trapping of the electron. The charge and its associated polarization cloud together form a polaron. Polaron formation confers semiconducting properties onto the polymer. In a simple particle in a box picture of electron delocalization along these segments, the energy of a polaron on a segment varies inversely with the segment length. Charges move around the film by hopping between these segments. This behavior differs dramatically from the localization observed in disordered inorganic semiconductors, such as hydrogenated amorphous silicon, where only states near the energy gap are strongly localized while all other states in the bands show significant delocalization over the entire structure [16]. Thus, the conventional bandlike description is not appropriate for amorphous polymers.

A bandgap of a few electron volts lies between the highest occupied molecular orbital (HOMO)—the lowest energy state from which an electron can be removed—and the lowest unoccupied molecular orbital (LUMO)—the lowest energy state at which an electron can be injected. When polarons bind together or an electron is excited by visible radiation from a HOMO to a LUMO level, the chain is deformed through electron–phonon interactions and an exciton is created with binding energies of 0.1–0.5 eV. The exciton self-traps to a region of the chain commonly referred to as a chromophore. When considering exciton motion, conjugated polymers are thus best described as a collection of weakly coupled chromophores with various conjugation lengths [20]. As with polarons, the energy associated with a chromophore is related to its length—the shorter the chromophore, the higher the energy. The resulting energetic disorder is usually referred to as inhomogeneous or static disorder. Energetic disorder also

arises owing to the screening or polarizing influences of the medium, with chromophores embedded in different local dielectric environments displaying distinct excitation energies. This picture has been corroborated, e.g., by the presence of multiple emission lines observed in ladder-type poly(p-phenylene)s using single molecule spectroscopy at cryogenic temperature [21]. In [21], it is shown that conjugated polymers whose chemical structure and hence electron–phonon interactions differ strongly both adhere to this picture, suggesting that it will apply to all conjugated polymers.

Unlike inorganic semiconductors, disorder in organic materials is not associated with broken chemical bonds. Disorder in polymer films has two origins: many stable conformations exist and intramolecular conformations lead to variations in bond lengths, torsional angles, and on-chain defects, whereas intermolecular interactions arise from material morphology, chain alignment, and packing. The molecular structure can result in amorphous and crystalline behavior. Small molecules can form crystals with long range order, favorable for high-mobility semiconductors for organic transistors. In polymer OLEDs, however, long range order in the form of polycrystalline domains can lead to exciton quenching and instability (crystallization with time can lead to device changes), so for these devices an amorphous morphology is preferable.

To develop molecular materials with improved transport properties, new techniques are needed to distinguish the relative roles of intrinsic polymer properties, e.g., conformation, packing, and polaron binding energy, and extrinsic factors in determining the nature of charge transport and the resulting mobilities. Experimental efforts to separate these factors, e.g., [22], can be aided by the approaches we have developed in [12] and [14].

III. CHARGE MIGRATION IN RIGID ROD CONJUGATED POLYMERS

We will describe how we made the first steps towards linking charge mobilities with chemical structure and morphology [12] for PFO, a blue emitting conjugated polymer of practical interest for light emission that has one of the highest μ_h yet reported for a conjugated polymer: $\mu_h \sim 10^{-3} - 10^{-2}$ cm^2/(Vs).

Several frameworks, such as the Gaussian disorder model (GDM) [23] and its variants, have been used to analyze the field and temperature dependences of mobility in disordered semiconductors. The GDM provides an expression for the temperature and electric field dependence of μ_h in terms of disorder in transport site energies and in hopping rates using Monte Carlo (MC) simulations of a biased random walk on disordered cubic lattices, often using the phenomenological Miller–Abrahams intersite hopping rate. Although the GDM has been used for comparative analysis of experimental data, it does not show how to predict charge transport properties from the physical and chemical structure of real molecular materials because the Miller–Abrahams rate parameters cannot be calculated directly from the chemical structure and because explicit information on the positions of charge transport units is excluded.

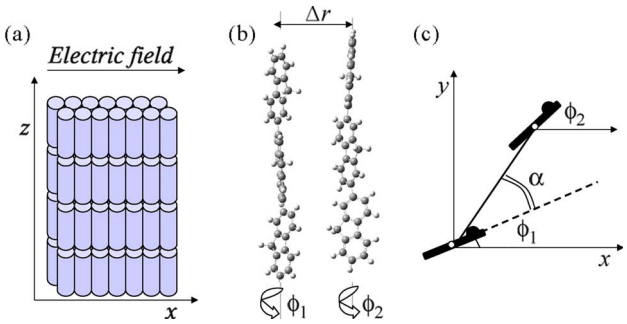

Fig. 3. *(a) Model morphology for aligned polymer chains. Each column contains trimers stacked end-to-end. (b) A pair of neighboring PFO trimers (C atoms are shown by dark spheres and H atoms by light spheres) showing interchain separation Δr and torsion angles φ. The octyl side chains are replaced by H atoms for the calculation of J and i. (c) Top view of the central planes of two trimers, showing the torsion angles φ_1 and φ_2 ($\Delta\varphi = \varphi_2 - \varphi_1$) and the polar angle α. (Taken from [12].)*

Like the GDM, our method employs Monte Carlo simulations of a biased random walk to model charge transport, but the hopping takes place on an arrangement of charge transporting units that is based on the observed structure of the crystalline PFO material, namely, a hexagonal lattice of lattice constant a where the chains are parallel both to each other and to the substrate, as illustrated in Fig. 3(a). A trimer of fluorene with a length of 2.3 nm, shown in Fig. 3(b), is the charge transporting unit in all cases: the trimer is the oligomer of length closest to the spatial extent of polarons in other polymers. Charge transporting units in conjugated polymers are expected to be of varying length and may vary dynamically in position and size through thermal fluctuations. Here, we restrict attention to a static lattice and to the case of trimers only, in order to focus on the effects of positional and torsional disorder without invoking energetic disorder due to varying segment length. For this preliminary work, we assumed a nearly ordered morphology since simulating realistic disordered morphologies for molecular materials on length scales comparable to device thicknesses and thus involving $\sim 10^6$ hopping sites is a challenging problem [24]. In any case, it is important to isolate the different factors affecting the mobility before trying to attempt an all-encompassing model.

We employed an approximate version [25] of small-polaron hopping rates calculated directly from the electronic structure of the units based on nonadiabatic

Marcus–Hush theory [16] for the intermolecular hole transfer rate between conjugated segments i and j

$$\Gamma_{ij} = \frac{2\pi}{\hbar} J_{ij}^2 \frac{1}{\sqrt{4\pi\lambda k_B T}} \exp\left\{ -\frac{(\Delta G_{ij} - \lambda)^2}{4\lambda k_B T} \right\} \quad (1)$$

where J_{ij} is the electronic transfer integral, λ is the molecular reorganization energy (equal to half the polaron binding energy), ΔG_{ij} is the free energy difference between initial and final sites, k_B is Boltzmann's constant, and T the temperature. The relaxed geometry of the trimer and the quantities J_{ij} and λ were obtained by quantum chemical techniques. The electronic coupling term J_{ij}^2 was shown to be very sensitive to chain separation $\Delta \boldsymbol{r}$ and relative dihedral angle $\Delta\varphi$ and the polar angle α [12].

The following cases were addressed:

i) an ordered morphology, where all trimers are located on lattice points with the same torsion angle φ [defined in Fig. 3(b)];

ii) a torsionally disordered system, where φ is distributed at random in the range 0 to 2π;

iii) a regular system, called the optimally ordered case, where relative torsion angles are chosen to maximize the net transfer rate in the field direction.

Lateral disorder was simulated via random lateral trimer displacements in the x–y plane taken from a uniform distribution, with a minimum separation of 0.63 nm to allow for excluded volume. We chose $a = 0.65$ nm with $\boldsymbol{F}$ directed along the x-axis. Introducing lateral disorder or disorder in slip had little effect on the μ_h of the torsionally disordered system at this chain separation. A waiting time τ_{ij} is calculated for a hop from site i to each of its six interchain and two intrachain nearest neighbor sites j from $\tau_{ij} = -\ln(X)/$¡ij, where X is a random number uniformly distributed between zero and one. The hop with the smallest τ_{ij} is executed and the simulation time advanced by τ_{ij}. In a procedure chosen to mimic the way in which mobilities are deduced from time-of-flight experiments [26], we find the average transit time $\langle\tau\rangle$ for several hundred hole trajectories where each hole is started at a randomly chosen trimer in the film and allowed to travel a fixed distance d, typically ten cell widths in the field direction. The simulated hole mobility $\mu_h = d/(\langle\tau\rangle F)$.

Fig. 4 shows μ_h for several morphologies in the Poole–Frenkel ($\log(\mu_h)$ versus $F^{1/2}$) representation widely used for experimental mobility data compared to experiment [26]. For a torsionally ordered system, the largest mobility values occur for molecular orientations where the trimers are not parallel. Results from an optimally ordered morphology are shown in Fig. 4. By allowing the unit cell more than one trimer, such that $\Delta\varphi = 150°$ for nearest neighbors along the $+x$ direction and $\Delta\varphi = 180°$ for $\alpha = 60°$, an unexpected consequence is that the torsionally disordered system leads to a μ_h approximately ten times larger than the ordered

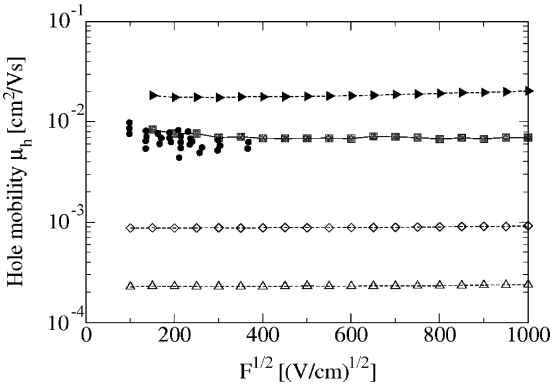

Fig. 4. *Poole–Frenkel plot for predicted μ_h compared to experimental data [26] (•) in an aligned PFO film at $T = 300$ K and a fixed interchain separation $\Delta r = a = 0.65$ nm, where F is parallel to x. Predicted μ_h values are shown for the ordered system devised to maximize μ_h (filled right triangles); the ordered system with fixed $\varphi = 20°$ (◊), with fixed $\varphi = 0°$ (△) and a lateral and torsionally disordered system (■). The lines are to guide the eye. (Taken from [12].)*

case with fixed $\varphi = 20°$, due to "sweet spots" where the interchain transfer rate is much higher than in the nonoptimal ordered case. Intrachain transport is much faster than interchain transport so pathways, termed "charge highways" [27], for fast charge transport are formed, linking these sweet spots. This result is a direct consequence of the one-dimensional nature of polymers, and the concept has since suggested a means of optimizing both charge mobility and optical properties of polymers, aiding the possibility of electrically pumped polymer lasers [11]. We infer that unless polymer films with the "right sort of order"—in other words, an optimally ordered morphology—can be grown, some disorder in the film is desirable for rapid charge transport. The variation of the coupling J_{ij}^2 with the chain orientation and separation and the reorganization energy λ and hence $\mu_h(F)$ in ordered systems will depend on the chemical structure. We are presently investigating this topic, along with the effects of energetic disorder. A much harder question to answer is how changes in chemical structure affect $\mu_h(F)$ through its sensitivity to disorder in the morphology since, as noted above, simulating realistic disordered morphologies for molecular materials on length scales comparable to device thicknesses is a problem beyond the scope of present-day computers. Thus we do not claim that we can predict device performance based on knowledge of the chemical structure, as is possible for some crystalline inorganic systems.

The result that less-ordered films have higher mobilities has been seen in measurements on polyhexathiophene using a combination of atomic force microscopy (AFM) with neutron scattering data [27]. Here, it was shown that chains form rod-like crystals at low molecular weight (MW) and the mobility in these materials is limited by poor connectivity and insulating grain boundaries between misoriented neighboring crystals, but at medium

and high MW, chains are longer than the grains and so minimize the effect of grain boundaries by bridging the domains. Earlier work by the authors of [28] using X-ray diffraction also showed that the relationship between charge transport and morphology is key to increasing the charge carrier mobility of conjugated polymers [29].

Morphological and electronic properties of thin films can be studied with a nanoscale resolution by combining AFM and Kelvin probe force microscopy (KPFM). KPFM allows quantitative mapping of the electronic properties of nanostructures through determination of the surface potential of nanoobjects with a lateral resolution less than 70 nm. Thus it is possible to see charge percolation paths, defects, and bottlenecks within the film [30]. The resulting contact potential domain structures from the lamellar regions in polythiophene have been seen with a combination of electrostatic force microscopy and KPFM [31]. Interpretation of all the measurements outlined in this paragraph requires the modeling approach we have developed where the morphology is explicitly allowed for. Our approach, unlike the GDM, could be used to interpret experimental data in the common situation of films characterized by structural heterogeneities, since the parameters obtained by a GDM analysis of these samples would not relate to transport parameters within the different domains in the films and would therefore have no useful physical meaning [22].

IV. EXCITON MIGRATION IN RIGID ROD CONJUGATED POLYMERS

As noted in Section I, exciton diffusion is important in determining the width of the recombination zone in OLEDs and hence color and lifetime. We have adapted the multiscale approach described above for charge transport to look at spectral diffusion and determine the exciton diffusion length L_D, namely, how far on average an exciton travels before recombining on an explicit polymer morphology.

Section II noted that, from the point of view of exciton motion, conjugated polymers can be described as a collection of weakly coupled chromophores with a distribution of conjugation lengths and hence energies. In optical absorption measurements on polymer films, vibrational modes are smeared out since light is absorbed by molecules/segments with different conformations. The created excitons lose energy as they move to chromophores of lower energy, the phenomenon of spectral diffusion. Emission samples a smaller distribution of conformations so more vibronic character is seen in emission spectra, especially in more ordered materials. Spectral diffusion was seen in Monte Carlo random walk simulations of exciton hopping made with the GDM (i.e., excitons hop between sites on a simple cubic lattice with semiphenomenological transfer rates) [32], but this approach is limited by the need to fit key parameters such as the Förster radius.

A model that can separate out the influence of energetic disorder from spatial chain arrangement on exciton migration is needed to link the chemical structure of the polymer, morphology, and optical and electronic properties. For example, it is useful to identify the contributions to exciton diffusion arising from intrachain (i.e., along the chains) and from interchain (i.e., between chains) energy migration. In [13], it was shown that intrachain processes dominate in solution where energy transfer is known from spectroscopic data to be rather slow. In films, close contacts between chains favor interchain transport, and this process is characterized by an order-of-magnitude increase in transfer rate with respect to solution. This description was supported by quantum-chemical calculations for exciton transfer rates that go beyond the usual point-dipole model approximation and account for geometric relaxation phenomena in the excited state before energy migration. The calculations indicate a two-step mechanism for intrachain energy transfer with hopping *along* the conjugated chains as the rate-limiting step; the higher efficiency of the interchain transfer process is due both to larger electronic coupling matrix elements between closely lying chains and to the larger phase space, i.e., there are more possibilities (six) for interchain hopping than for intrachain hopping (two).

We employed the exciton transfer rate methodology described in [13] to simulate exciton hopping on an ensemble of chains of poly-(6,6′, 12,12′ − tetraalkyl−2, 8-indenofluorene) (PIF) at 7 and 294 K [14]. PIF is a step-ladder blue emitting polymer promising for optoelectronic device applications. We adopted a simple ordered morphology for the polymer chains in which they are all aligned parallel to the z-axis and form a hexagonal lattice with a lattice constant of 1 nm taken from X-ray data. There were three stacks of chains. Each chain was modelled as a group of 11 rigid rods of varying length, as the total length of the group is that of a typical polymer chain. The chromophore length distribution was taken from experimental absorption spectra. By averaging over the Monte Carlo trajectories such as the trajectory shown in Fig. 5, we were able to track the evolution of the excited chromophore length distribution.

Fig. 6 shows how our predicted zero to one photoluminescence peak energy evolves. High-energy chromophores relax by moving downhill in energy space and low-energy chromophores through moving uphill until a stationary state is reached. The increase in energy arises for low-energy chromophores because the available thermal energy exceeds the energy barrier from the site energy mismatch due to the different conjugation lengths. In the long time limit, the predicted mean excitation energy of the zero to one peak converges to the experimental value (2.72 eV). This value is slightly higher than the thermodynamic limit due to the finite excited-state lifetime.

Theoretical data (not shown in Fig. 6) yielded significantly higher relaxation rates than experiment [33], so we chose sites on our ordered morphology at random to be traps. At these sites, the transfer rate into the site was a hundred times larger and the transfer rate out of the site a hundred times smaller than the transfer rates had it not

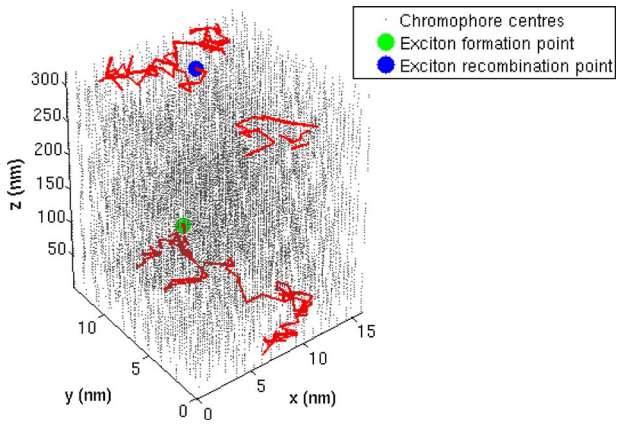

Fig. 5. *Trajectory of an exciton created at the point (5, 10, 100) that recombines at the point (10, 10, 300) on an ordered chain morphology. Note that periodic boundary conditions have been used. (Taken from [14].)*

been a trap site. Evidence for traps comes from red-shifted photoluminescence emission seen in many spectra that can be explained by delocalization of the excitons in regions where the chromophores aggregate [34]. The role of these interchain species has been hard to establish because materials processed under different conditions will have different morphologies. It is likely that these aggregates are sites that act as traps. In [14], we ignored the detailed nature of the traps and, for a specified trap concentration, chose sites on our ordered morphology at random to be traps. By including traps, the time-evolution of the predicted average emission energy is close to the experimental data. The presence of traps does not affect strongly the first 10 ps since the probability for finding a nontrap site is high. At longer times, however, the electronic excitations that are attracted by the trap centers with larger Förster radii compared to nontrap sites stay in those traps, slowing down the relaxation process.

Our predictions for the diffusion length L_D for different trap concentrations and for 1-D (intrachain) diffusion are shown in Fig. 7. Our results can be explained by the competition between hopping and decay. In chains or at low temperatures, a hop takes a time typically longer than the time for radiative decay, so the excitons decay before they can find a trap. Without traps, $L_D \sim 45$ nm, about one order of magnitude larger than the experimental values reported so far for conjugated polymers of 10 nm or less but close to diffusion lengths reported for small molecules and semiconducting carbon nanotubes—see Table 2 and references cited in [14]. It only takes a trap concentration of 0.5% for L_D to decrease from 45 to 15 nm. Inhomogeneous broadening of the chromophore spectra due to the random environment may also explain why we predict faster energy relaxation times and longer L_D values than the experiment. Our model can take this broadening into account using relevant experimental input, and we find it does have a significant effect on L_D.

Our results for three-dimensional motion fulfill the analytical theory of Montroll [35] that does not include exciton recombination, showing that, unlike 1-D, the exciton transport is so fast that most excitons find the traps before they decay, a result that could not be easily foreseen. An elegant analytical approach has been developed for exciton diffusion to carrier centers where dissociation occurs to explain experimental data on the kinetics of charge photogeneration [36]. It relies on the concepts discussed above, namely, energy relaxation and the competition

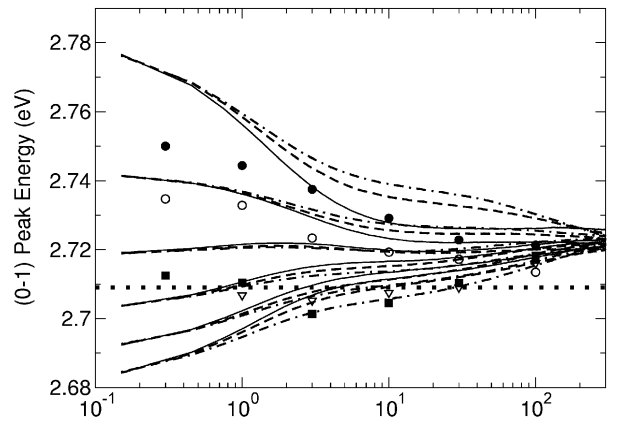

Fig. 6. *Mean zero to one emission peak energy E_{01} versus time t. Each curve corresponds to a given starting site length, in descending order: 3-mers, 4-mers, 5-mers, 6-mers, 7-mers, and 8-mers. Experimental results [33] at excitation energies in electron volts of 3.062 (filled circles), 2.962 (empty circles), 2.884 (diamonds), and 2.851 (triangles) are also shown. Here, temperature T = 294 K and homogeneous line width $\Gamma = 0.04$ eV; solid lines: 0.5% traps; dashed lines: 1% traps; dashed-dotted lines: 1.5% traps. The dotted line shows the thermodynamic limit. (Taken from [14].)*

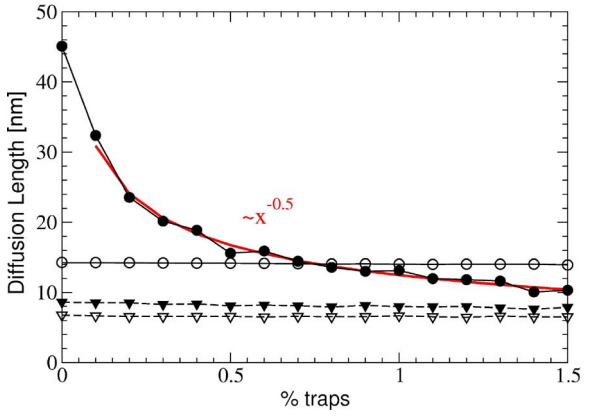

Fig. 7. *L_D variation with the percentage of sites occupied by traps x. Solid lines: T = 294 K; dashed lines T = 7 K. Filled circles indicate intra- and interchain hops permitted; empty circles are for intrachain hops only. The line showing L_D varies as $x^{0.5}$ comes from the prediction of [35]. (Taken from [14].)*

between hopping, decay, and finding a dissociation center. By combining this analytical model with the Monte Carlo model described in this section, we have shown that energetic disorder plays an important role as it slows down diffusion and its presence is sufficient to limit the values of exciton diffusion length even in the absence of positional disorder [37]. Therefore, the underlying reason limiting exciton diffusion in conjugated polymers might be related to the disorder in these materials. This disorder causes a variation in the chromophore energies that is much greater than electronic interaction energy promoting exciton delocalization and transport and is seen in all conjugated polymer films regardless of their chemical structure and solid-state packing, including semicrystalline material with high charge carrier mobilities.

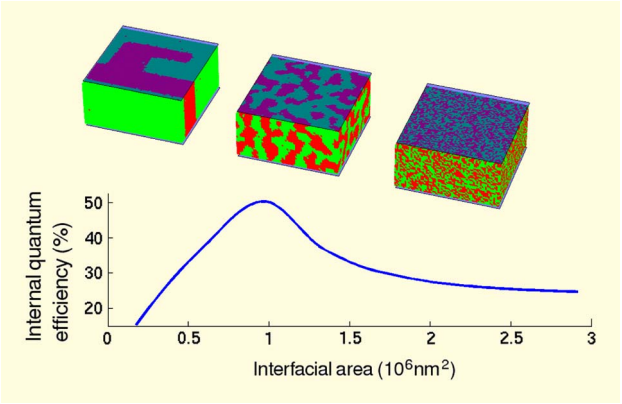

Fig. 8. *Internal quantum efficiency (%) versus interfacial area (10^6 nm^2) and example morphologies generated by minimization of an Ising Hamiltonian. Electron and hole conductors are displayed as dark (red in color plot) regions and light (green in color plot) regions, respectively. The anode and cathode (blue in color plot) are the top and bottom planes and are separated by 90 nm. (Table of contents plot from [41].)*

V. DEVICE MODELS

Conventional device models adapted from inorganic device simulation have given strong insights into OLED behavior at macroscopic length scales—for recent examples, see [38] and [39]—and they have been reviewed along with the GDM in [40]. The hopping nature of conduction in organic materials discussed in Section II is taken into account by the use of field-dependent charge mobilities obtained from experiment. It is likely that these inorganic device models work well, even though the conventional band-like description implicit in such models is not valid because some averaging must take place on the 100-nm length scale relevant to these devices and because the Coulomb interactions between the charges are treated correctly. A disadvantage of using the device models is the large number of parameters that have to be fitted to experiment, as discussed in [40]. A better approach would be to use the predicted charge mobilities and exciton diffusion coefficients from the simulations described in Sections III and IV, respectively, instead of experimental values in the device models. In this way, we can extend our models from the mesoscopic description in Sections III and IV to a macroscopic level.

Most OLEDs consist of planar layers of material ~10 nm thick. For adequate light absorption in organic photovoltaics, the thickness of material that can absorb light is ~100 nm, since the polymers and dyes used for light harvesting have light absorption coefficients of $\sim(100\ \text{nm})^{-1}$ in the visible part of the spectrum. The light generates excitons, which have to separate into free charges before they recombine. The photogenerated charges have to be extracted from the electrodes before they in turn recombine. As noted in Section III, the diffusion length, the typical distance travelled before recombination, can be much less than this thickness for excitons or charges.

To reduce the likelihood of exciton recombination, the hole and electron conducting phases interpenetrate on a nanometer scale, creating a so-called bulk heterojunction. Excitons can then reach an interface between the two phases before they recombine. In dye-sensitized cells, this problem is addressed by using a third phase, a monolayer of dye molecules, as the light harvesting medium and placing the dye layer at the bulk heterojunction. For all the organic cells, the use of a bulk heterojunction increases the probability that the photogenerated charges recombine. If electron and hole conductors interpenetrate on a small scale, charge separation is efficient but charge transport may be inhibited. Conversely, when electron and hole conductors exist in larger phases and interpenetrate less, charge transport may be enhanced but exciton dissociation diminished. When a bulk heterojunction is employed, there is therefore a tradeoff between efficient dissociation of excitons and loss-free charge transport. This tradeoff is seen for the internal quantum efficiency, the ratio of the number of charges extracted to the number of photons absorbed, in Fig. 8. This prediction was obtained from a device model by my group [41] and since extended [42]–[44]. It is based on the dynamical Monte Carlo (DMC) approach. DMC allows simulation of charge and energetic processes in any morphology on the nanometer scale with charge mobilities and the exciton diffusion coefficients as input, and can easily be adapted to OLEDs.

On a coarser length scale, a less computationally resource-intensive continuum electrical/optical model has been developed for organic blend solar cells [45]. We have developed a two-dimensional continuum model so that we can treat the bulk heterojunction as two separate interpenetrating phases [46]. We have included the effects of optical interference shown in Fig. 9, exciton diffusion, charge separation via the formation of polaron pairs, and charge transport in two phases. Our model shows that the current is increased by an order of magnitude with a full optical model compared to assuming that absorbed

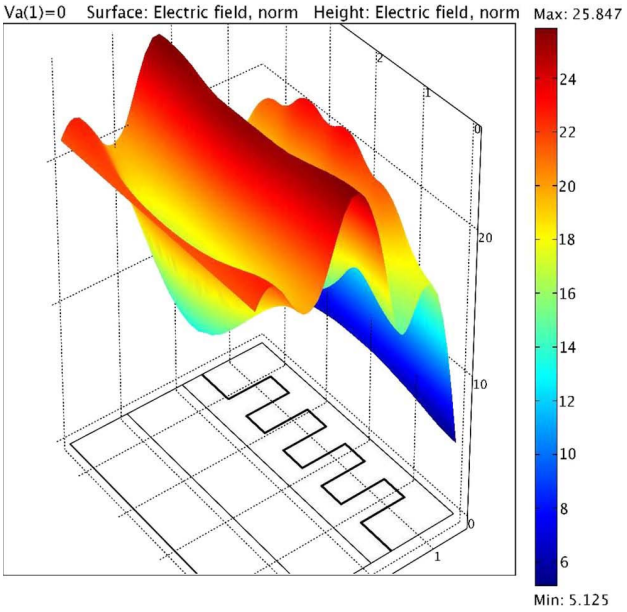

Fig. 9. *Example plot of the magnitude of the optical electric field (in Vm^{-1}, with values from 5.125 to 25.847 Vm^{-1}) inside a device at 0.1 Sun. The figure also shows the underlying device morphology. (Taken from [46].)*

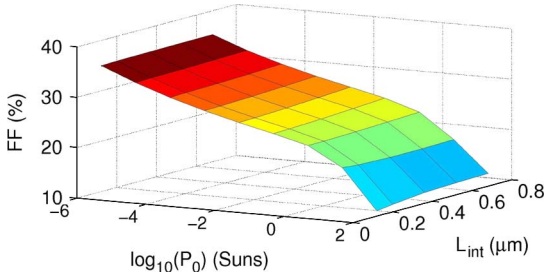

Fig. 10. *Fill factor as a function of intensity (Suns) and interface length. (Taken from [46].)*

photons have a Lambertian profile, and depends much more strongly on applied bias when dissociation via polaron pairs is considered. We find a power efficiency at solar intensities of 1–3% depending on the morphology. Fig. 10 shows that the fill factor, the ratio of the maximum obtainable power (the power output at the point on the current–voltage characteristic where the power is maximum) to the theoretically possible power (the product of the open-circuit voltage and short circuit current), decreases from 37% at low intensities to 20% at solar intensities because of the increase in the open-circuit voltage and decreases much more rapidly at higher intensities due to the decrease in the power efficiency.

VI. CONCLUSIONS AND NEXT STEPS

We have investigated the links between charge and exciton transport and the chain packing in organic polymers, a subject of much debate in experimental groups because of its scientific interest and technological implications but that is only just starting to be addressed theoretically. Much has been learned in approximate morphologies by considering the difference between inter- and intrachain transport. The next step for our charge transport simulations will be to include energetic disorder by considering a distribution of conjugate segment lengths. This task is a straightforward extension of our model but is far more resource-intensive. Employing more realistic polymer film morphology would be interesting, although a morphology using interatomic forces obtained from the chemical structure for the system sizes required is extremely hard. Another sticking point is the extent that domain boundaries between ordered regions and extrinsic effects such as impurities dominate the mobilities. Regarding exciton transport, we are now using the same techniques as in [14] to look at exciton diffusion on a group of indenofluorene trimers. Packing arrangements of the trimers are obtained from molecular dynamics calculations in an extension of studies of energy transport predictions on this system.

We have also developed device models that employ the output from our mesoscale modelling to look at larger length scales. These models are based on Monte Carlo and drift diffusion methods, the former being relevant for the 10-nm length scale and the latter for length scales of 100 nm to 1 μm. These approaches share with the mesoscale modelling the ability to link charge and energy transport with morphology, a feature that is increasingly important for interpretation of the extensive body of experimental work on organic devices and for exploitation of the devices made from them. ■

Acknowledgment

Special thanks are owed to the coauthors of [12] and [14], S. Athanasopoulos, D. Beljonne, J. Nelson, C. Foden, J. Kirkpatrick, J. Frost, E. Hennebicq, and D. Martínez.

REFERENCES

[1] C. W. Tang and S. A. VanSlyke, "Organic electroluminescent diodes," *Appl. Phys. Lett.*, vol. 51, p. 913, 1987.

[2] R. H. Friend, R. W. Gymer, A. B. Holmes, J. H. Burroughes, R. N. Marks, C. Taliani, D. D. C. Bradley, D. A. Dos Santos, J. L. Brédas, M. Lögdlund, and W. R. Salaneck, "Electroluminescence in conjugated polymers," *Nature*, vol. 397, p. 121, 1999.

[3] J. Shinar and R. Shinar, "Organic light-emitting devices (OLEDs) and OLED-based chemical and biological sensors: An overview," *J. Phys. D, Appl. Phys.*, vol. 41, p. 133001, 2008.

[4] Z. Bao, "Organic materials for thin film transistors *Material Matters*, vol. 2. St. Louis, MO: Sigma-Aldrich, 2007, pp. 4–6.

[5] R. Capelli, F. Dinelli, M. A. Loi, M. Murgia, R. Zamboni, and M. Muccini, "Ambipolar organic light-emitting transistors employing heterojunctions of n-type and p-type materials as the active layer," *J. Phys., Condens. Matter*, vol. 18, pp. S2127–S2138, 2006.

[6] T. Kietzke, "Recent advances in organic solar cells," *Adv. Optoelectron.*, vol. 2007, 2007, art 40285.

[7] C. Buchgraber, A. Pogantsch, S. Kappaun, J. Spanring, and W. Kern, "Luminescent copolymers for applications in

multicolor-light-emitting devices," *J. Poly. Sci. A*, vol. 44, pp. 4317–4327, 2006.

[8] S. Difley, D. Beljonne, and T. Van Voorhis, "On the singlet-triplet splitting of geminate electron—Hole pairs in organic semiconductors," *J. Amer. Chem. Soc.*, vol. 130, pp. 3420–3427, 2008.

[9] E. Polikarpov and M. E. Thompson, "Achieving high efficiency in organic light-emitting devices," *Material Matters*, vol. 2. St. Louis, MO: Sigma-Aldrich, 2007, pp. 21–23.

[10] R. Street, "The benefit of order," *Nature Mater.*, vol. 5, pp. 171–172, 2006.

[11] B. K. Yap, R. Xia, M. Campoy-Quiles, P. N. Stavrinou, and D. D. C. Bradley, "Simultaneous optimisation of charge carrier mobility and optical gain in semiconducting polymer films," *Nature Mater.*, vol. 7, pp. 376–380, 2008.

[12] S. Athanasopoulos, J. Kirkpatrick, D. Martínez, J. M. Frost, C. M. Foden, A. B. Walker, and J. Nelson, "Predictive study of charge transport in disordered semiconducting polymers," *Nano Lett.*, vol. 7, pp. 1785–1788, 2007.

[13] D. Beljonne, G. Pourtois, C. Silva, E. Hennebicq, L. M. Herz, R. H. Friend, G. D. Scholes, S. Setayesh, K. Müllen, and J.-L. Brédas, "Interchain vs. intrachain energy transfer in acceptor-capped conjugated polymers," *Proc. Nat. Acad. Sci.*, vol. 99, pp. 10 982–10 987, 2002.

[14] S. Athanasopoulos, E. Hennebicq, D. Beljonne, and A. B. Walker, "Trap limited exciton transport in conjugated polymers," *J. Phys. Chem. C*, vol. 112, pp. 11532–11538, 2008.

[15] F. C. Grozema and L. D. A. Siebbeles, "Mechanism of charge transport in self-organizing organic materials," *Int. Rev. Phys. Chem.*, vol. 27, pp. 87–138, 2008.

[16] V. Coropceanu, J. Cornil, D. A. da Silva Filho, Y. Olivier, R. Silbey, and J.-L. Brédas, "Charge transport in organic semiconductors," *Chem. Rev.*, vol. 107, pp. 926–952, 2007.

[17] S. Kilina, E. R. Batista, P. Yang, S. Tretiak, A. Saxena, R. L. Martin, and D. L. Smith, "Electronic structure of self-assembled amorphous polyfluorenes," *ACS Nano*, vol. 2, pp. 1381–1388, 2008.

[18] J. Kirkpatrick, V. Marcon, J. Nelson, K. Kremer, and D. Andrienko, "Charge mobility of discotic mesophases: A multiscale quantum and classical study," *Phys. Rev. Lett.*, vol. 98, 2007.

[19] J. J. Kwiatkowski, Nelson, H. Li, J. L. Bredas, W. Wenzel, and C. Lennartz, "Simulating charge transport in tris(8-hydroxyquinoline) aluminium (Alq3)," *Phys. Chem. Chem. Phys.*, vol. 10, pp. 1852–1858, 2008.

[20] H. Bässler and B. Schweitzer, "Site-selective fluorescence spectroscopy of conjugated polymers and oligomers," *Acc. Chem. Res.*, vol. 32, pp. 173–182, 1999.

[21] F. Schindler, J. M. Lupton, J. Feldmann, and U. Scherf, "A universal picture of chromophores in π-conjugated polymers derived from single-molecule spectroscopy," *Proc. Nat. Acad. Sci.*, vol. 41, pp. 14 695–14 700, 2004.

[22] M. Sims, S. M. Tuladhar, J. Nelson, R. C. Maher, M. Campoy-Quiles, S. A. Choulis, M. Mairy, D. D. C. Bradley, P. G. Etchegoin, C. Tregidgo, K. Suhling, D. R. Richards, P. Massiot, C. B. Nielsen, and J. H. G. Steinke, "Correlation between microstructure and charge transport in poly(2,5-dimethoxy-p-phenylenevinylene) thin films," *Phys. Rev. B*, vol. 76, 2007.

[23] H. Bässler, "Charge transport in disordered organic photoconductors a Monte Carlo simulation study," *Phys. Status Solidi B*, vol. 175, pp. 15–56, 1993.

[24] D. Andrienko, V. Marcon, and K. Kremer, "Atomistic simulation of structure and dynamics of columnar phases of hexabenzocoronene derivatives," *J. Chem. Phys.*, vol. 125, 2006, art 124902.

[25] J. Kirkpatrick, "An approximate method for calculating transfer integrals based on the ZINDO Hamiltonian," *Int. J. Quantum Chem.*, vol. 108, pp. 51–56, 2008.

[26] T. Kreouzis, D. Poplavskyy, S. M. Tuladhar, M. Campoy-Quiles, J. Nelson, A. J. Campbell, and D. D. C. Bradley, "Temperature and field dependence of hole mobility in poly(9,9-dioctylfluorene)," *Phys. Rev. B*, vol. 73, 2006, art 235201.

[27] P. M. Borsenberger, L. Pautmeier, and H. Bässler, "Charge transport in disordered molecular solids," *J. Chem. Phys*, vol. 94, p. 5447, 1991.

[28] R. J. Kline and M. D. McGehee, "Morphology and charge transport in conjugated polymers," *Polymer Rev.*, vol. 46, pp. 27–45, 2006.

[29] R. J. Kline, M. D. McGehee, and M. F. Toney, "Highly oriented crystals at the buried interface in polythiophene thin-film transistors," *Nature Mater.*, vol. 5, pp. 222–228, 2006.

[30] A. Liscio, G. De Luca, F. Nolde, V. Palermo, K. Müllen, and P. Samorì, "Photovoltaic charge generation visualized at the nanoscale: A proof of principle," *J. Amer. Chem. Soc.*, vol. 130, pp. 780–781, 2008.

[31] B. Pérez-García1, J. Abad, A. Urbina, J. Colchero, and E. Palacios-Lidón, "Surface potential domains on lamellar P3OT structures," *Nanotechnology*, vol. 19, 2008, art 065709.

[32] S. C. J. Meskers, J. Hübner, M. Oestreich, and H. Bässler, "Dispersive relaxation dynamics of photoexcitations in a polyfluorene film involving energy transfer: Experiment and Monte Carlo simulations," *J. Phys. Chem. B*, vol. 105, pp. 9139–9149, 2001.

[33] L. M. Herz, C. Silva, A. C. Grimsdale, K. Müllen, and R. T. Phillips, "Time-dependent energy transfer rates in a conjugated polymer guest-host system," *Phys. Rev. B*, vol. 70, 2004.

[34] B. J. Schwartz, "Conjugated polymers as molecular materials: How chain conformation and film morphology influence energy transfer and interchain interactions," *Ann. Rev. Phys. Chem.*, vol. 54, pp. 141–172, 2003.

[35] E. W. Montroll, "Random walks on lattices containing traps," *J. Phys. Soc. Jpn. Suppl.*, vol. 26, pp. 6–10, 1969.

[36] V. Arkhipov, E. V. Emelianova, and H. Bässler, "On the role of spectral diffusion of excitons in sensitized photoconduction in conjugated polymers," *Chem. Phys. Lett.*, vol. 383, pp. 166–170, 2004.

[37] E. V. Emelianova, S. Athanasopoulos, A. B. Walker, and D. Beljonne, "Exciton diffusion in energetically disordered organic materials," *Phys. Rev. B.*, 2009, submitted for publication.

[38] S. G. Stevenson, I. D. W. Samuel, S. V. Staton, K. A. Knights, P. L. Burn, J. Williams, and A. B. Walker, "Current-voltage characteristics of dendrimer light-emtting diodes," *Synth. Metals*, 2009.

[39] S. L. M. van Mensfoort and R. Coehoorn, "Effect of Gaussian disorder on the voltage dependence of the current density in sandwich-type devices based on organic semiconductor," *Phys. Rev. B*, vol. 78, 2008, art 085207.

[40] A. B. Walker, A. Kambili, and S. J. Martin, "Electrical transport modelling in organic electroluminescent devices," *J. Phys. Condens. Matter*, vol. 14, pp. 9825–9876, 2002.

[41] P. K. Watkins, A. B. Walker, and G. L. B. Verschoor, "Dynamical Monte Carlo modelling of organic solar cells: The dependence of internal quantum efficiency on morphology," *Nano Lett.*, vol. 5, pp. 1814–1818, 2005.

[42] R. A. Marsh, C. Groves, and N. C. G. Greenham, "A microscopic model for the behavior of nanostructured organic photovoltaic devices," *J. Appl. Phys.*, vol. 101, 2007, art 083509.

[43] F. Yang and S. R. Forrest, "Photocurrent generation in nanostructured organic solar cells," *ACS Nano*, vol. 2, pp. 1022–1032, 2008.

[44] L. Meng, Y. Shang, Q. Li, Z. Shuai, R. G. E. Kimber, and A. B. Walker, "Dynamic Monte Carlo simulation for highly efficient polymer blend photovoltaics," *J. Amer. Chem. Soc.*, 2009, submitted for publication.

[45] S. Lacic and O. Inganäs, "Modelling electrical transport in blend heterojunction solar cells," *J. Appl. Phys.*, vol. 97, 2005, art 124901.

[46] J. Williams and A. B. Walker, "Two-dimensional simulations of bulk heterojunction solar cell characteristics," *Nanotechnology*, vol. 19, p. 424 011, 2008.

[47] C. Bacchiocchi, E. Hennebicq, S. Orlandi, L. Muccioli, D. Beljonne, and C. Zannoni, "Reduced distributed monopole model for the efficient prediction of energy transfer in condensed phases," *J. Phys. Chem. B*, vol. 112, pp. 1752–1760, 2008.

[48] T. Kietzke, "Highly efficient polymer light emitting diodes," *Polymer Rev.*, vol. 46, pp. 7–26, 2006.

[49] D. Andrienko, J. Kirkpatrick, V. Marcon, J. Nelson, and K. Kremer, "Structure-charge mobility relation for hexabenzocoronene derivatives," *Phys Stat. Sol. (b)*, vol. 245, pp. 830–834, 2008.

ABOUT THE AUTHOR

Alison B. Walker was born in Sarawak, Malaysia. She received the D.Phil. degree from the University of Oxford, U.K.

She was a Research Associate with Michigan State University, East Lansing, and Daresbury Laboratory, U.K., then took permanent posts first at the University of East Anglia, U.K., and next at the University of Bath, U.K. Her research focusses on modelling novel solar cells and organic devices. She held a Royal Society Industry Fellowship with Cambridge Display Technology. Currently she is Coordinator of the European Commission STREP project Modelling Electroactive Conjugated Materials at the Multiscale (MODECOM) and is part of the SUPERGEN Excitonic Solar Cell Consortium funded by the U.K. Engineering and Physical Sciences Research Council.